Aminobacter sp. MSH1 mineralises the groundwater micropollutant 2,6-dichlorobenzamide through a unique chlorobenzoate catabolic pathway

Bart Raes[1], Benjamin Horemans[1], Daniel Rentsch[2], Jeroen T'Syen[1], Maarten G. K. Ghequire[3], René De Mot[3], Ruddy Wattiez[4], Hans-Peter E. Kohler[5], Dirk Springael[1]*

[1] Division of Soil and Water management, Department of Earth and Environmental Sciences, Faculty of Bioscience Engineering, KU Leuven, Leuven, Belgium

[2] Laboratory for Functional Polymers, Empa, Swiss Federal Laboratories for Materials Science and Technology, Dübendorf, Switzerland

[3] Centre of Microbial and Plant Genetics, KU Leuven, Leuven, Belgium

[4] Department of Proteomics and Microbiology, University of Mons, Mons, Belgium

[5] Department of Environmental microbiology, Eawag, Swiss Federal Institute of Aquatic Science and Technology, Dübendorf, Switzerland

* Corresponding author: Division of Soil and Water management, Department of Earth and Environmental Sciences, Faculty of Bioscience Engineering, Kasteelpark Arenberg 20, KU Leuven, Leuven, Belgium; Tel. 32 16 32 16 04;

Fax 32 16 32 19 97; e-mail: dirk.springael@kuleuven.be

Table of contents

Sodium dodecyl sulphate polyacrylamide gel electrophoresis (SDS-PAGE). Ten µL of each crude protein extract, which were brought to the same protein contents, was mixed in equal volume with protein loading dye (20 % SDS, 20 % glycerol, 20 mM tris-HCl pH 6.8, 2 mM EDTA pH 7.0, 260 mM dithiothreitol) and incubated at 95°C for 10 min followed by 5 min incubation at 4°C. The mixtures were loaded on a Mini-PROTEAN TGX precast gel (Biorad) with the Precision Plus Protein™ Unstained Standards ladder (Biorad) as a protein size marker. Electrophoresis was performed for 50 min at 200 V in electrophoresis buffer (200 mM glycine, 3.5 mM SDS, 25 mM tris-HCl, pH 8.3). The gel was rinsed three times with ultrapure water, stained for 60 min with SimplyBlue™ SafeStain (Invitrogen) and destained with ultrapure water (60 min).

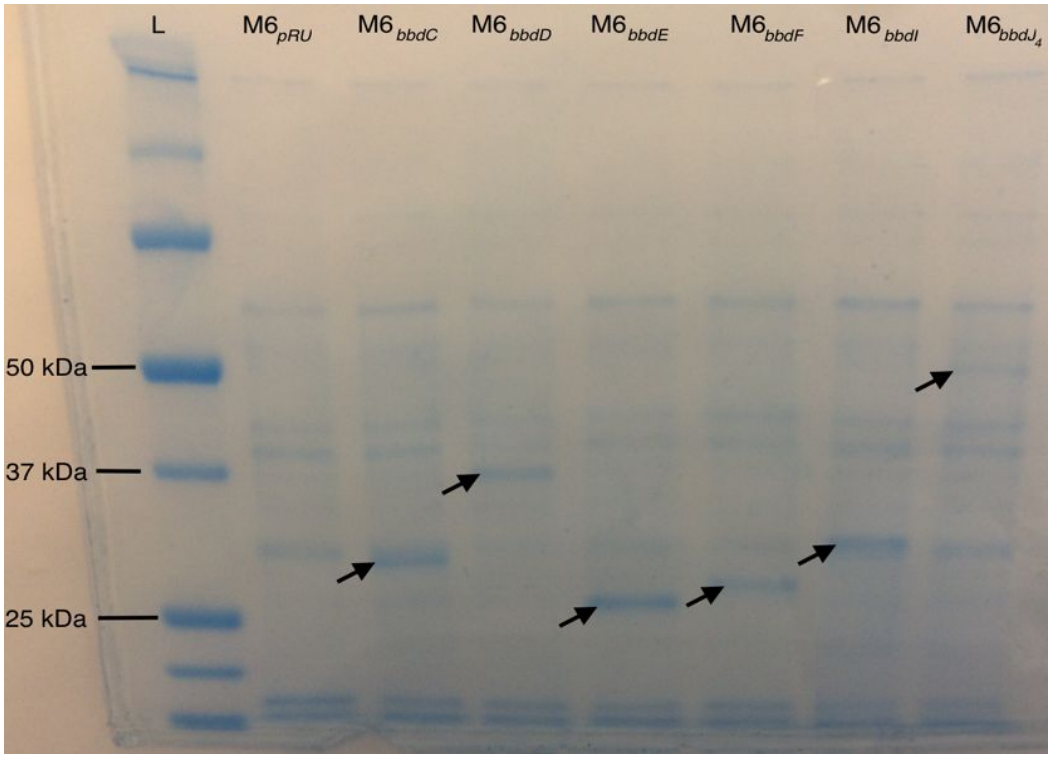

Figure S1. SDS-PAGE of crude protein extracts of the M6.100g variant carrying the empty pRU1097 vector ($M6_{pRU}$) and of the M6.100g variants $M6_{bbdC}$, $M6_{bbdD}$, $M6_{bbdE}$, $M6_{bbdF}$, $M6_{bbdI}$ and $M6_{bbdJ4}$ carrying pRU1097 derivatives containing the pBAM2 catabolic genes *bbdC, bbdD, bbdE, bbdF, bbdI or* $bbdJ_4$, respectively, all under the control of the constitutive promoter of *bbdA*. Equal amounts of proteins from each crude extract were loaded on the gel. The lanes are indicated accordingly; Lane L: Precision Plus Protein™ Unstained Standards ladder. The arrows show the corresponding Bbd proteins.

Isolation and identification of BbdC by anion exchange (AEC) and hydrophobic interactions chromatography (HIC). A crude protein extract of MSH1 wt, grown in 1 L MS medium supplemented with 5 mM BAM at 25°C, was prepared in 20 mL lysis buffer. The crude extract was dialysed to a buffer containing 20 mM Tris and 20 mM NaCl (pH 8.0) overnight. AEC and HIC were performed on a Äkta purifier (GE Healthcare). For AEC, a HiTrap Q HP anion exchange column (GE Healthcare) and flow rates of 1 mL min^{-1} were used. After column equilibration with running buffer (20 mM NaCl, 20 mM Tris at pH 8.0) for 5 min, the sample was loaded and proteins were eluted with a linear gradient of NaCl (20 mM to 1 M in 20 mM Tris, pH 8.0) over 60 min. Proteins were collected in 2 mL fractions and analysed for 2-Cl-3,5-diOHBA conversion by adding 0.1 volumes to MS medium containing 500 µM 2-Cl-3,5-diOHBA. Time lapse 200 µL samples were taken, acidified with 2 µL of 37 % HCl and centrifuged (21380 *x g*, 5 min) and 170 µL of the supernatant was used to determine the remaining 2-Cl-3,5-diOHBA concentration by RP-UHPLC. HIC was applied on the pooled active fractions from AEC. The sample was supplemented with ammonium sulphate buffer (1.7 M, 20 mM Tris, pH 7.5) to a final concentration of 1 M ammonium sulphate. HIC was performed using a HiTrap phenyl sepharose HP column (GE Healthcare) and a flow rate of 1 mL min^{-1}. After column equilibration with running buffer (1 M ammonium sulphate, 20 mM Tris, pH 7.5) for 10 min, the sample was loaded and proteins eluted with a linear gradient of ammonium sulphate (1 M to 0 M in 20 mM Tris, pH 7.5) over 90 min. Proteins were collected in fractions of 2 mL and tested for conversion of 2-Cl-3,5-diOHBA as described above. After HIC, fractions were analysed with SDS-PAGE, to check protein purity. Proteins in active fractions were identified by LC-MS/MS as described by Breugelmans *et al* [1].

Preparation of pathway intermediates for identification by LC-MS/MS, GC-MS and NMR. Preparation of metabolites for UHPC-MS/MS analysis: Pathway intermediates were analysed by LC-MS/MS directly after UHPLC separation except for compounds A, B and C obtained from conversion of 2,6-diCl-3-OHBA by the MSH1 wt culture. Compounds A, B and C were first purified from the culture upon 80 % of 2,6-diCl-3-OHBA conversion. To this end, the culture was centrifuged (6000 *x g*, 15 min, 15°C), the supernatant filtered using a 0.2 µm filter (Fisherbrand), the filtrate concentrated using a RC 900 Rotary Evaporator (KNF) to a volume of 2 mL, and the concentrate acidified with 20 µL of 37 % HCl. Metabolites were purified from the acidified concentrate with RP-UHPLC by collecting and pooling relevant fractions from 250 µl injections and the pooled fractions were analysed by LC-MS/MS.

Preparation of pathways intermediates for GC-MS analysis: GC-MS was used for additional identification of the conversion product of 2,3,5-triOHBA by the $M6_{bbdF}$ crude protein extract. To this end, fifty mL of supernatant was acidified with HCl below pH 2 and extracted twice with 25 mL of ethyl acetate. The sample was dried over sodium sulfate and the volume was reduced to 1 mL by blowing off with nitrogen. Subsequently, 0.5 ml *N*, *O*-Bis(trimethylsilyl)trifluoroacetamide (BSTFA) was added for derivatization and the mixture was heated for 15 min at 70°C.

Preparation of metabolites for NMR analysis: NMR analysis of compounds A, B and C obtained from conversion of 2,6-diCl-3-OHBA by MSH1 wt, was performed on the pooled UHPLC fractions mentioned above after complete evaporation in the RC 900 Rotary Evaporator (KNF) and subsequent dissolution in either 250 µL methanol-d_4 (compounds A and C) or 250 µL DMSO-d_6 (compound B). NMR analysis of the product of 2,6-DCBA conversion by $M6_{bbdD}$ cells was performed after 70 % conversion of the substrate. The reaction mixture was centrifuged (6000 *x g*, 15 min, 18°C), filtered through a 0.2 µm filter (Fisherbrand), acidified with HCl to pH 2.0, extracted with twice with ethyl acetate, completely evaporated (RC 900 Rotary Evaporator, KNF), and dissolved in 250 µL methanol-d_4. The same procedure was used for NMR analysis of compounds D and F obtained from the conversion of 2-Cl-3,5-diOHBA by the $M6_{bbdC}$ protein extract and the conversion of 2,3,5-triOHBA by the $M6_{bbdF}$ protein extract, respectively. After evaporation, Compound D was dissolved in 250 µL DMSO-d_6 and compound F in 650 µL

D2O/DMSO-d6 5/1. NMR analysis of authentic compounds was performed after dissolution in either methanol-d_4 or DMSO-d_6 (as indicated in Tables S2 and S3) at a concentration of 100 mM.

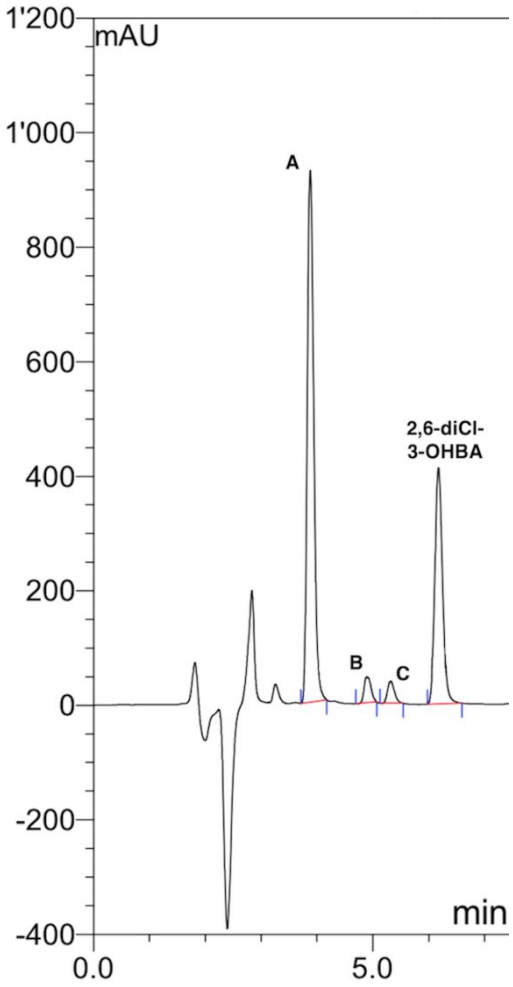

Figure S2. RP-UHPLC chromatogram of the supernatant of MSH1 wt cells incubated with 2,6-diCl-3-OHBA. The horizontal axis shows the retention time in minutes, the vertical axis displays the UV absorbance at 210 nm in mAU units. Degradation of 2,6-diCl-3-OHBA was concomitant with the appearance of three degradation products (compounds A, B and C).

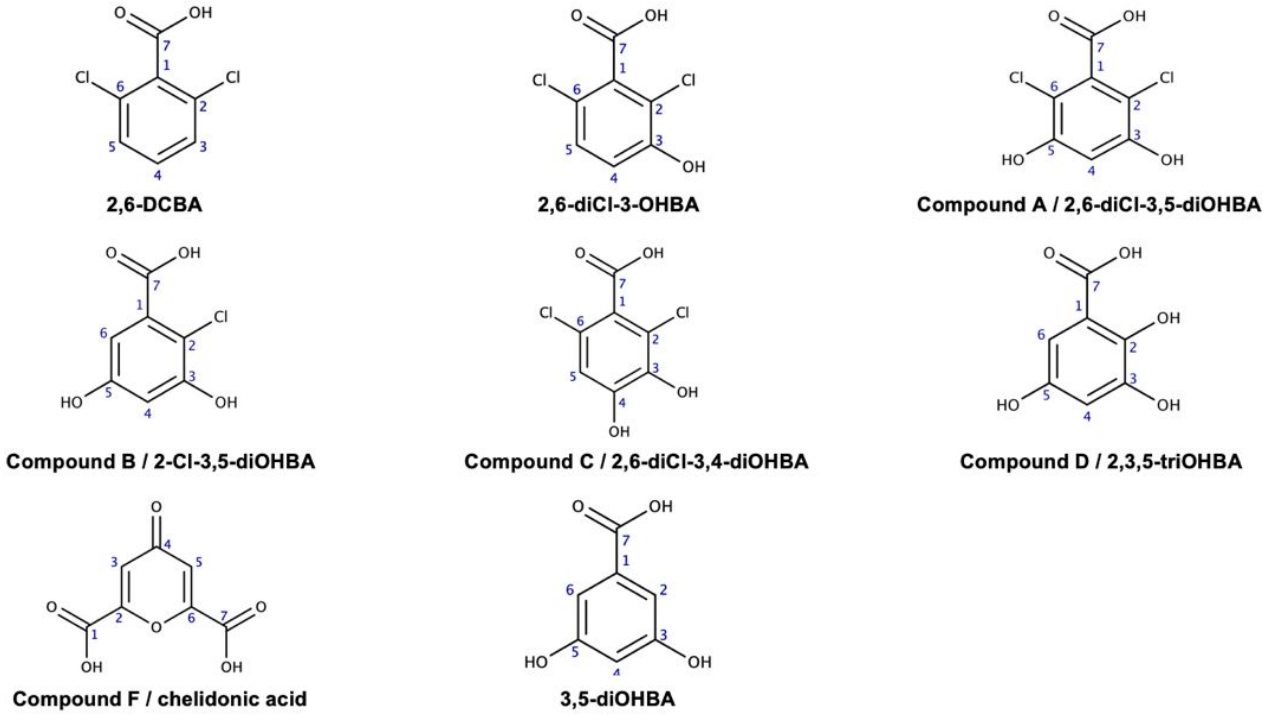

Figure S3. Chemical structures of 2,6-DCBA and its pBAM2 pathway intermediates showing their carbon atom numbers used in NMR signal assignments as reported in Tables S2 and S3.

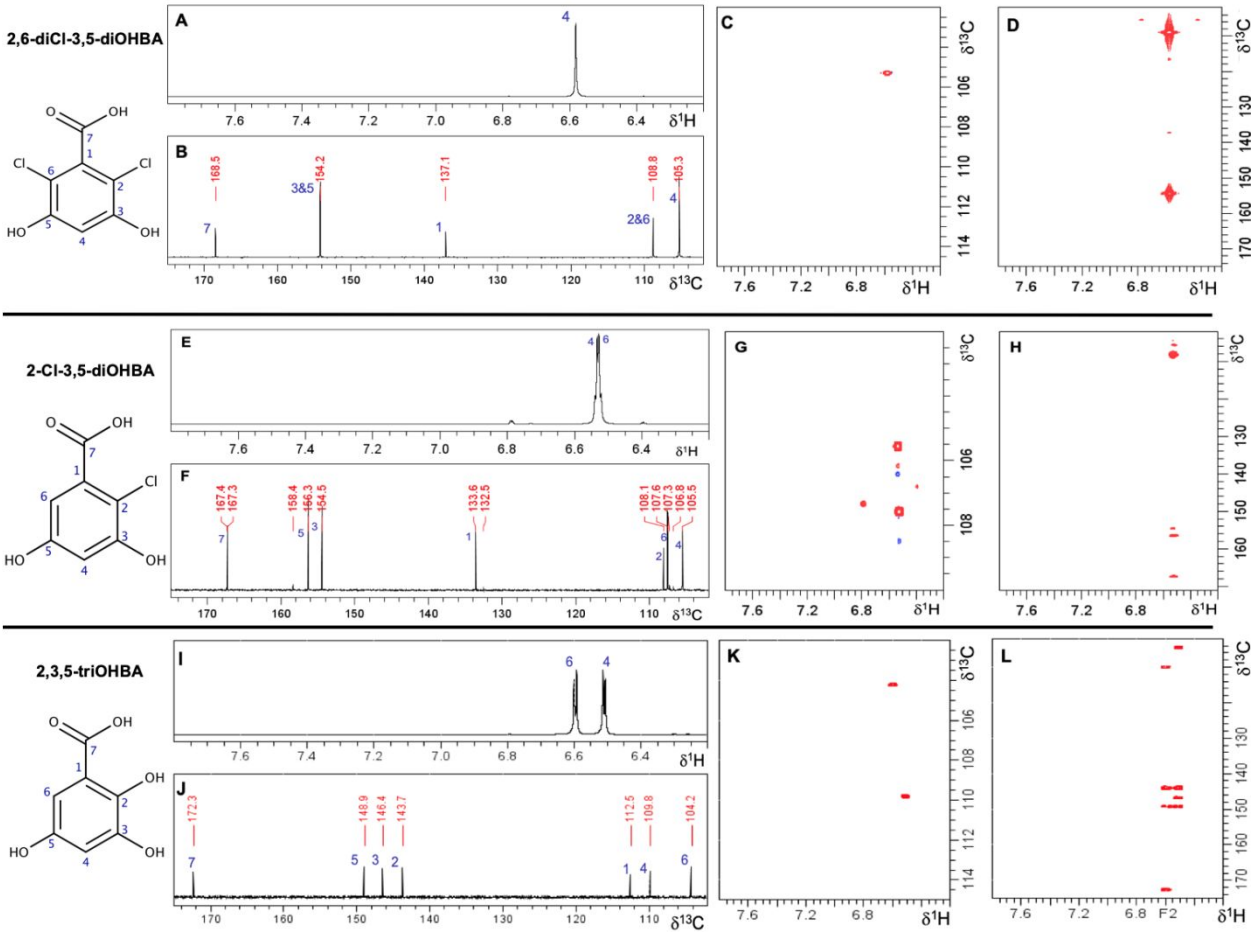

Figure S4. NMR data with signal assignments (in blue) to chemical structures of authentic 2,6-diCl-3,5-diOHBA (recorded in methanol-d_4), 2-Cl-3,5-diOHBA and 2,3,5-triOHBA (both recorded in DMSO-d6). ^{1}H NMR spectra are depicted in panels (A), (E) and (I), ^{13}C NMR spectra in (B), (F) and (J), ^{1}H-^{13}C HSQC spectra in (C), (G) and (K) and ^{1}H-^{13}C HMBC NMR spectra in (D), (H) and (L). Authentic 2-Cl-3,5-diOHBA contained approximately 2 % of 3,5-diOHBA as impurity. This explains the additional signals of 6.39 and 6.78 ppm in the ^{1}H NMR spectrum (E) and resonances at 106.8 ppm, 107.3 ppm, 132.5 ppm, 158.4 ppm and 167.4 ppm in the ^{13}C NMR spectrum (F).

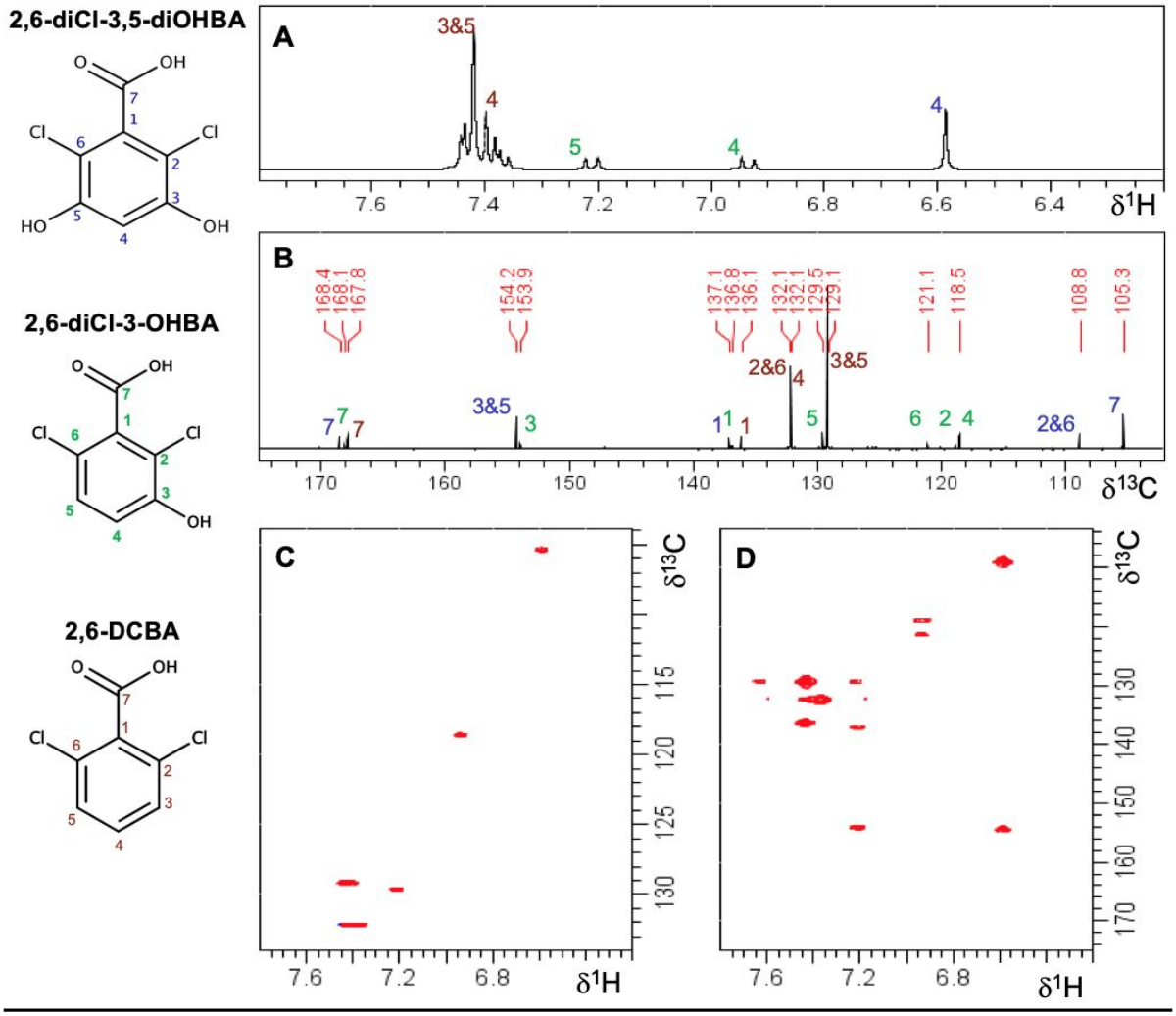

Figure S5. NMR data (recorded in methanol-d_4) of 2,6-diCl-3,5-diOHBA and 2,6-diCl-3-OHBA produced by M6$_{bbdD}$ cells from 2,6-DCBA as a substrate with signal assignments in blue, green and brown, respectively. ^{1}H NMR spectrum (A), ^{13}C NMR spectrum (B), ^{1}H-^{13}C HSQC NMR spectrum (C) and ^{1}H-^{13}C HMBC NMR spectrum (D). From ^{1}HNMR a molar ratio of 59:11:30 mol/mol-% of 2,6-DCBA/2,6-diCl-3-OHBA/2,6-diCl-3,5-diOHBA was determined.

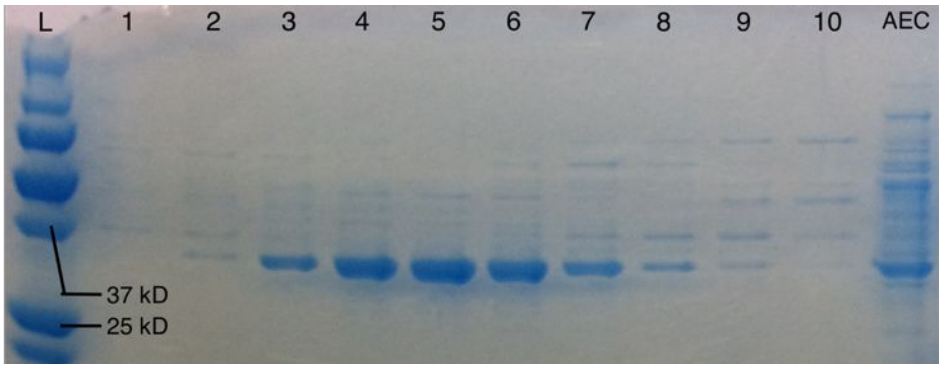

Figure S6. SDS-PAGE of collected protein fractions obtained by a combination of AEC and HIC from a crude protein extract of wild type *Aminobacter* sp. MSH1 grown on 1 mM BAM (Lanes 1-10). Lane L: Precision Plus Protein™ Unstained Standards ladder; AEC: pooled active fractions after anion exchange chromatography. Fractions 2 to 9 showed conversion of 2-Cl-3,5-diOHBA.

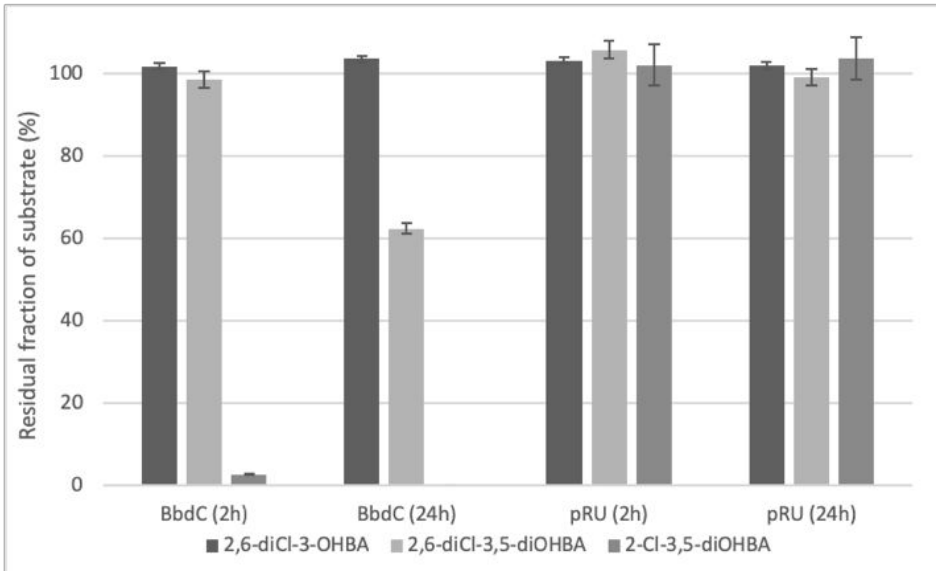

Figure S7. Fractions of 2,6-diCl-3-OHBA, 2,6-diCl-3,5-diOHBA and 2-Cl-3,5-diOHBA remaining after 2- and 24-hours incubation with crude protein extracts of $M6_{bbdC}$ (BbdC) and $M6_{pRU}$ as negative control (pRU). Values are averages with indicated standard deviation (n=2).

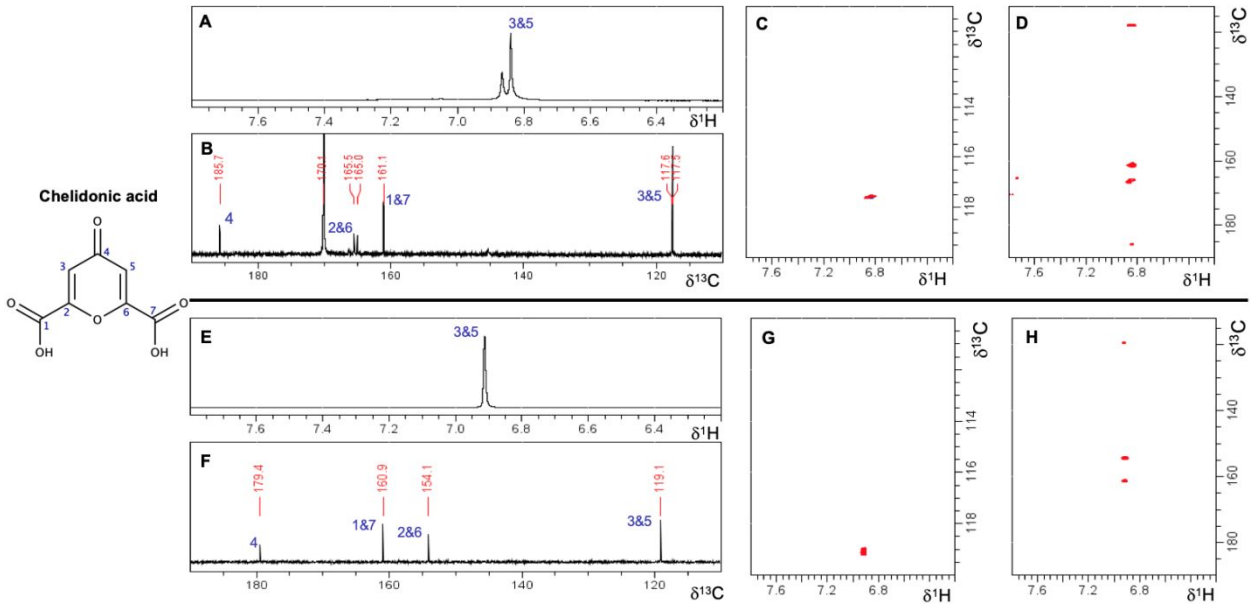

Figure S8. NMR data of compound F ([M-H]- ion of m/z 183.10) produced by BbdF from 2,3,5-triOHBA (in D2O/DMSO-d6 5/1, panels A-D) and authentic chelidonic acid (recorded in DMSO-d6, panels E-F). ^{1}H-NMR spectrum in panel (A, E), ^{13}C-NMR spectrum in (B, F), ^{1}H-^{13}C HSQC spectrum in (C, G) and ^{1}H-^{13}C HMBC spectrum in (D, H).

For compound F, the singlet signal at 6.84 ppm in the ^{1}H NMR spectrum (panel A) showed a correlation with a carbon at 117.5 ppm in the ^{1}H-^{13}C HSQC spectrum (panel C; Table S2). Since a correlation at 6.84/117.5 ppm is found in the ^{1}H-^{13}C HMBC spectrum as well (panel D), compound F must be symmetric, having two CH groups being separated by only one (or none) carbon. Furthermore, correlation signals were found to carbons at 185.7 ppm, 165.5 ppm, 161.1 ppm (Table S2). The set of five ^{13}C NMR signals indicated a symmetrical molecule and therefore the presence of chelidonic acid was suspected.

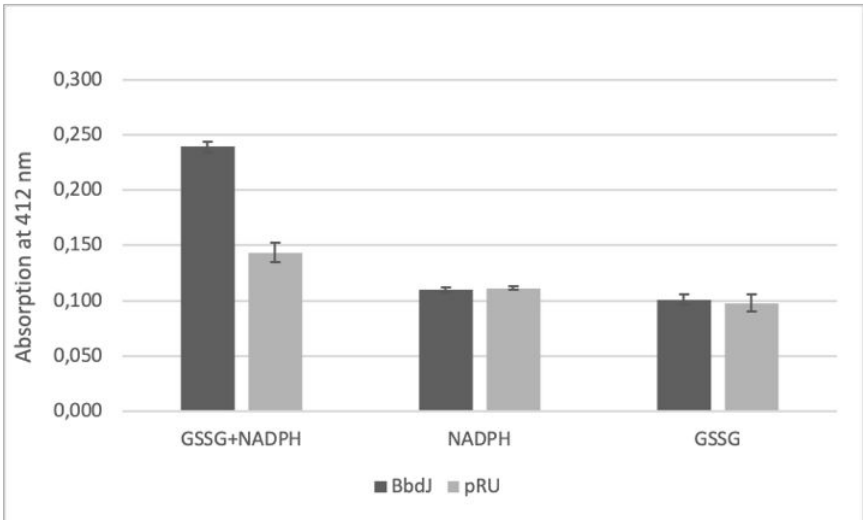

Figure S9. Glutathione reducing activity of $BbdJ_4$ in crude protein extracts of $M6_{bbdJ4}$ (BbdJ) and $M6_{pRU}$ (pRU) supplemented with both 1 mM GSSG and 1 mM NADPH, only 1 mM NADPH or only 1 mM GSSG. The GSSG conversion rate was 25.48 µmol.$mg_{total\ protein}^{-1}$.h^{-1}. Values are averages with indicated standard deviation (n=3).

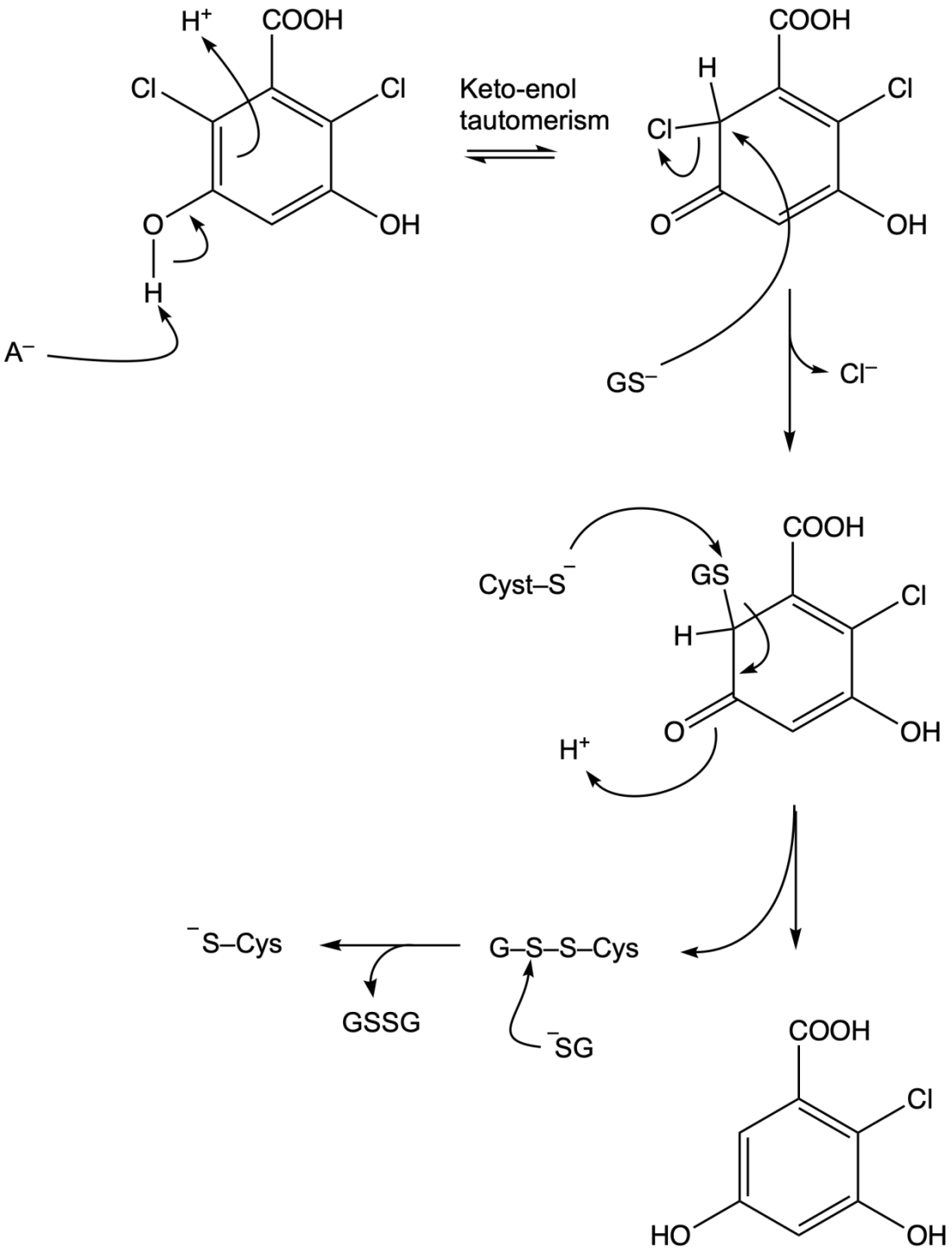

Figure S10. Suggested dehalogenation mechanism of BbdI and BbdE on 2,6-diCl-3,5-diOHBA in analogy with the mechanism of PcpC on TCHQ in *Sphingobium chlorophenolicum* as postulated by Warner *et al*. [2].

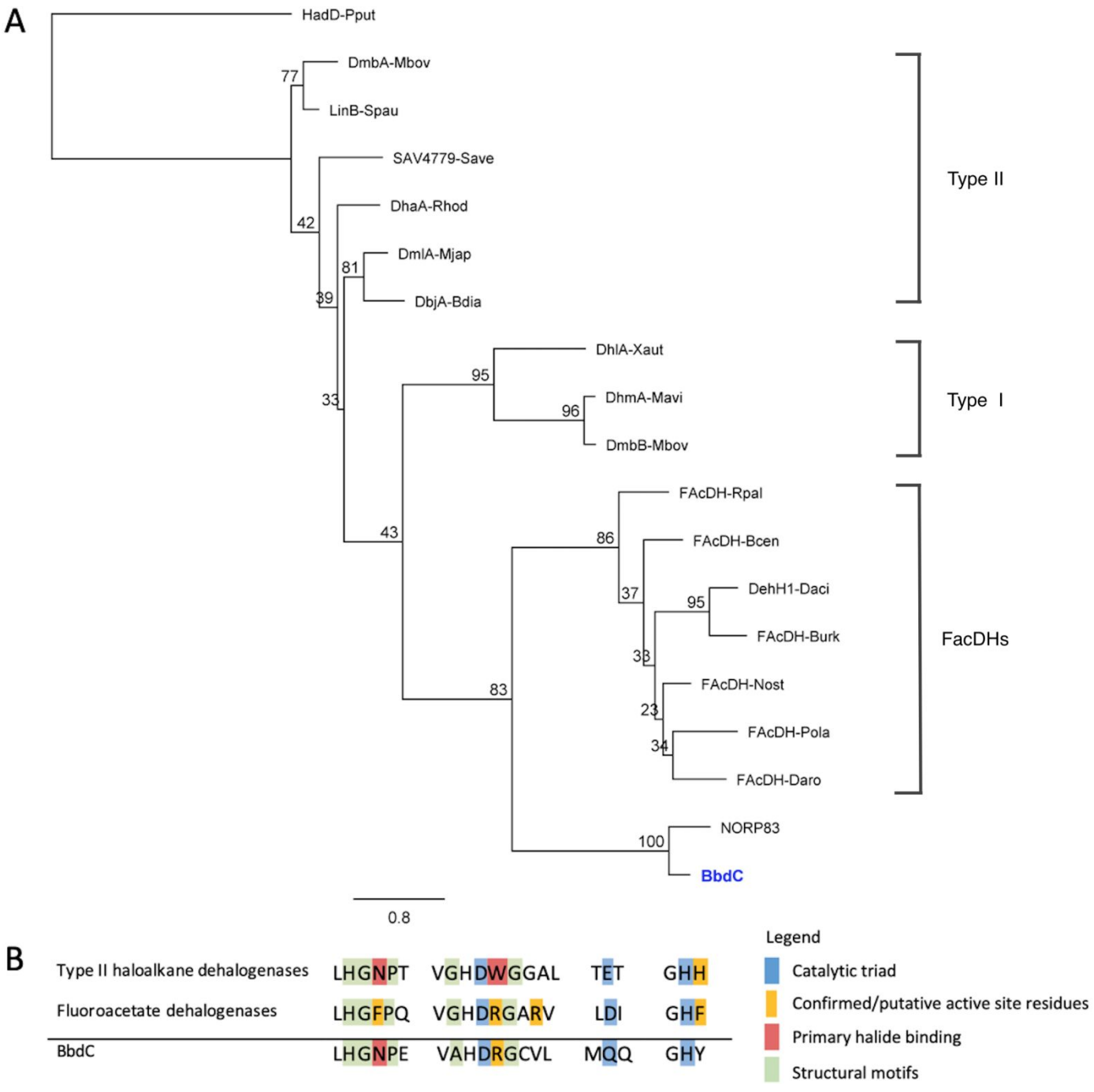

Figure S11. (A) Phylogeny of BbdC and related hydrolytic dehalogenases. Maximum likelihood phylogenetic tree (PhyML, JTT substitution model; Geneious 11.1.3) inferred from the multiple alignment of amino acid sequences homologous to residues 40-286 of BbdC (A0A1V0M576). The scale bar represents 0.8 substitutions per site. Bootstrap values (percentages of 1000 replicates) are shown at the branches. The tree is rooted to D-2-haloacid dehalogenase of *Pseudomonas putida* (HadD-Pput; Q52086). Sequences of other known dehalogenases included are: (i) Type I

haloalkane dehalogenases of *Mycobacterium avium* N85 (DhmA-Mavi; CAC41377), *Mycobacterium bovis* 5033/66 (DmbB-Mbov; CAH04660) and *Xanthobacter autotrophicus* GJ10 (DhlA-Xaut; AAA88691); (ii) Type II haloalkane dehalogenases of *Bradyrhizobium diazoefficiens* USDA110 (DbjA-Bdia; BAC46352), *Mesorhizobium japonicum* MAF303099 (DmlA-Mjap; Q98C03), *M. bovis* 5033/66 (DmbA-Mbov; CAH04659), *Rhodococcus* sp. (DhaA-Rhod; P59336), *Sphingomonas paucimobilis* (LinB-Spau; P51698) and *Streptomyces avermitilis* MA-4680 (SAV4779-Save; BAC72491); (iii) fluoroacetate dehalogenases of *Burkholderia cenocepacia* HI2424 (FAcDH-Bcen; ABK09712.1), *Burkholderia* sp. FA1 (FAcDH-Burk; Q1JU72), *Dechloromonas aromatica* RCB (FAcDH-Daro; Q479B8), *Delftia acidovorans* (DehH1-Daci; Q01398), *Nostoc* sp. PCC 7120 (FAcDH-Nost; Q8Z0Q1), *Polaromonas* sp. JS666 (FAcDH-Pola; Q123C8) and *Rhodopseudomonas palustris* CGA009 (FAcDH-Rpal; Q6NAM1). The putative BbdC homologue designated 'NORP83' is retrieved from the metagenome sequence of an uncharacterized marine OCS116-cluster α-Proteobacterium [3].

(B) Characteristic amino acid diagnostic motifs of type II haloalkane dehalogenases and fluoroacetate dehalogenases (according to Chan *et al.* [4]) and of BbdC. BbdC displays deviations from these diagnostic motifs at the active site and cannot be accurately assigned to one of the existing subtypes. Type I and II haloalkane dehalogenases possess a Trp at the nucleophile +1 position while FAcDHs contain an Arg. For BbdC, this residue is also an Arg. However, at the nucleophile +4 position, BbdC contains a Val instead of another Arg like FAcDHs. Also, BbdC carries a Gln as part of its predicted catalytic triad D-Q-H whereas FAcDHs contain an Asp and type II dehalogenases a Glu. The protein of NORP83 related to BbdC also shows the D-Q-H predicted catalytic triad.

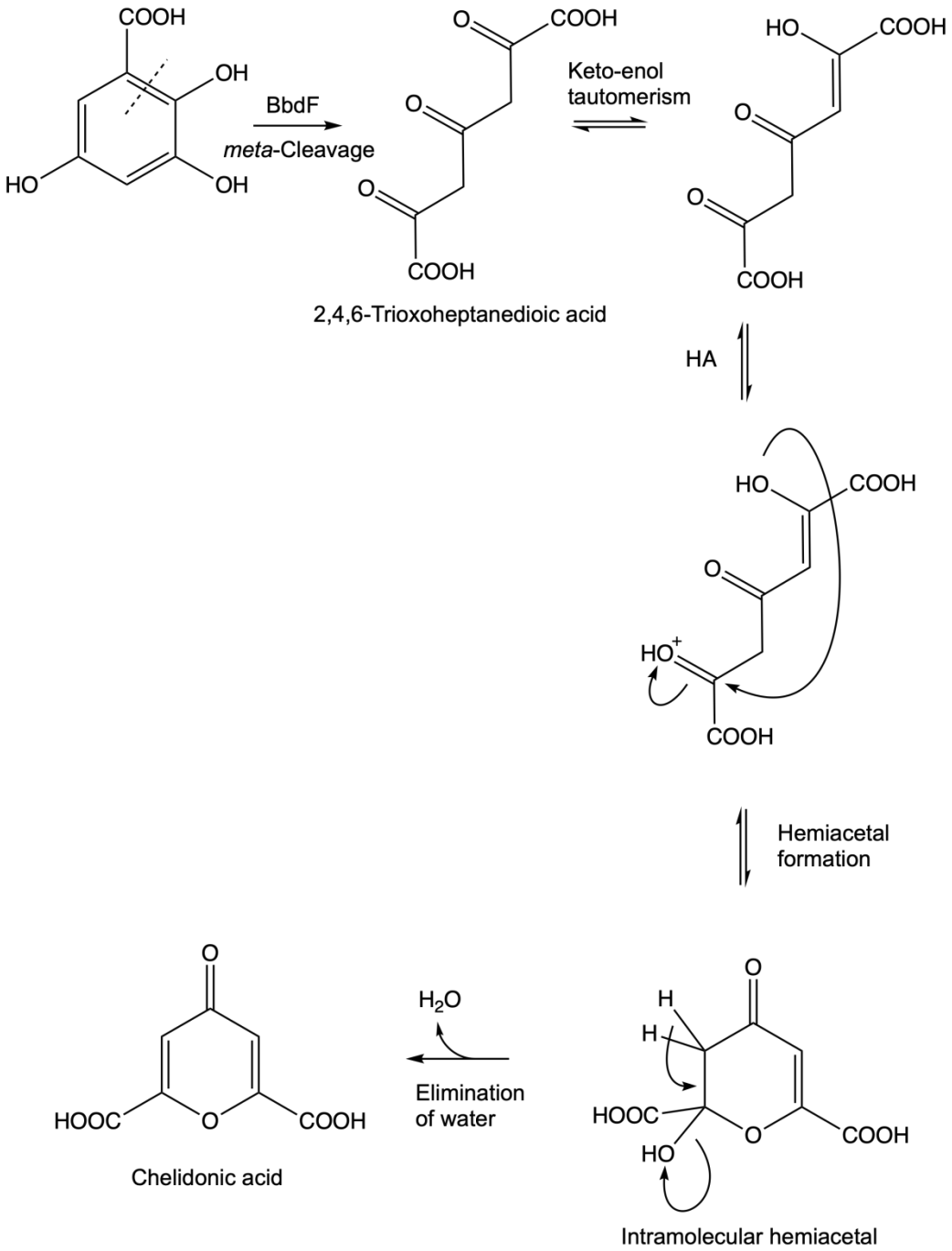

Figure S12. Putative pathway for the formation of chelidonic acid observed in incubations of crude extracts of M6$_{bbdF}$ with 2,3,5-triOHBA as the substrate. 2,3,5-triOHBA is cleaved by BbdF yielding 2,4,6-trioxoheptanedioic acid, which exist as an equilibrium mixture of several tautomers. Protonation of a keto group allows for easy formation of an intramolecular hemiacetal. Subsequently, water is eliminated to form chelidonic acid as has been postulated for biosynthesis of chelidonic acid in cultured plant cells [5].

Table S1. Overview of full MS and MS^2 scans with the most abundant *m/z* values of the compounds A, B, C, D and E by means of LC-MS/MS. All measurements were conducted in the negative ionization mode.

	m/z	Relative peak intensity	Identification of MS signals
		Compound A	
MS	220.94	100 %	$[M-H]^-$, $C_7H_3{}^{35}Cl_2O_4$
	222.94	62 %	$[M-H]^-$, $C_7H_3{}^{35}Cl^{37}ClO_4$
	224.94	10 %	$[M-H]^-$, $C_7H_3{}^{37}Cl_2O_4$
MS^2	176.95		$[M-H-CO_2]^-$
	140.97		$[M-H-CO_2-{}^{35}Cl]^-$
	105.00		$[M-H-CO_2-{}^{35}Cl_2]^-$
		Compound B	
MS	186.98	100 %	$[M-H]^-$, $C_7H_4{}^{35}ClO_4$
	188.98	32 %	$[M-H]^-$, $C_7H_4{}^{37}ClO_4$
MS^2	142.99		$[M-H-CO_2]^-$
	107.01		$[M-H-CO_2-{}^{35}Cl]^-$
	63.02		
		Compound C	
MS	220.94	100 %	$[M-H]^-$, $C_7H_3{}^{35}Cl_2O_4$
	222.94	62 %	$[M-H]^-$, $C_7H_3{}^{35}Cl^{37}ClO_4$
	224.94	10 %	$[M-H]^-$, $C_7H_3{}^{37}Cl_2O_4$
MS^2	176.95		$[M-H-CO_2]^-$
	140.95		$[M-H-CO_2-{}^{35}Cl]^-$
	105.00		$[M-H-CO_2-{}^{35}Cl_2]^-$
	77.00		
		Compound D	
MS	169.10		$[M-H]^-$, $C_7H_5O_5$
MS^2	125.20		$[M-H-CO_2]^-$
	107.15		$[M-H-CO_2-OH-H]^-$
	79.15		
		Compound E[(a)]	
MS	201.10		$[M-H]^-$, $C_7H_5O_7$
MS^2	129.20		
	57.15		

		41.15

222 [a] Analysis of compound E prior to storage and preparation for NMR.

Table S2. ^{1}H NMR chemical shift assignments, coupling constants (*J*) and ^{1}H-^{13}C NMR long range correlations in methanol-d4 and DMSO-d6 solutions, molecular weights and chemical formulas of detected isolated metabolites and of corresponding authentic compounds. Numbering of carbon atoms for all compounds is shown in Figure S3.

Compound	MW (g/mole)	Chemical formula	$\delta^{1}H$ (ppm)	position / No. of H	Coupling pattern [(a)] / *J* (Hz)	Observed ^{1}H-^{13}C HMBC correlations (ppm; w=weak)	Remark
methanol-d_4							
Isolated metabolites							
2,6-diCl-3-OHBA	207.01	$C_7H_4Cl_2O_3$	7.21	5 / 1H	d / 8.8	168.1w/153.9/136.8/121.1	Produced by M6$_{bbdD}$ cells
			6.93	4 / 1H	d / 8.8	153.9/121.1/118.8	
Compound A	223.01	$C_7H_4Cl_2O_4$	6.51	4 / 1H	s	154.0/108.6	Produced by MSH1 wt
Compound C	223.01	$C_7H_4Cl_2O_4$	6.74	5 / 1H	s	170.9w/147.5/142.4/131.2/120.5/ 118.6w	Produced by MSH1 wt
Authentic compounds							
2,6-DCBA	191.01	$C_7H_4Cl_2O_2$	7.42	3&5 / 2H	m	167.7w/136.0/129.1	Substrate for M6$_{bbdD}$ cells
			7.39	4 / 1H	m	132.2	
2,6-diCl-3-OHBA	207.01	$C_7H_4Cl_2O_3$	7.21	5 / 1H	d / 8.8	168.1w/153.9/136.8/121.1/118.8 w	Substrate for MSH1 wt
			6.93	4 / 1H	d / 8.8	153.9/136.8w/121.1/118.8	
2,6-diCl-3,5-diOHBA	223.01	$C_7H_4Cl_2O_4$	6.58	4 / 1H	s	154.2/137.1w/108.8	
2-Cl-3,5-diOBA	188.56	$C_7H_5ClO_4$	6.69	6 / 1H	d / 2.8	169.8/157.8/110.7/101.7	
			6.53	4 / 1H	d / 2.8	157.8/155.8/134.1w/110.7/109.6	

3,5-diOHBA	154.12	$C_7H_6O_4$	6.78	2&6 / 2H	d / 2.2	170.0/159.7/109.0/108.1	By-product of authentic 2-Cl-3,5-diOHBA
			6.39	4 / 1H	t / 2.2	159.7	
DMSO-d_6							
Isolated metabolites							
Compound B	188.56	$C_7H_5ClO_4$	6.45	6 / 1H	d / 2.8	168.1/156.3w/107.8/104.9	Produced by MSH1 wt
			6.48	4 / 1H	d / 2.8	156.3/154.8/107.8/107.2	
Compound D	170.12	$C_7H_6O_5$	6.59	6 / 1H	d / 2.9	172.3/148.9w/143.6/109.8	Produced by purified BbdC
			6.51	4 / 1H	d / 2.9	148.9w/146.4w/143.6/104.1	
Compound F [(b)]	184.10	$C_7H_6O_7$	6.84	3&5 / 2H	s	185.7w/165.5w/161.1/117.5	Produced by $M6_{bbdF}$ extract
Authentic compounds							
2-Cl-3,5-diOHBA	188.56	$C_7H_5ClO_4$	6.52	6 / 1H	d / 2.8	167.3/156.3/108.1/105.5	
			6.53	4 / 1H	d / 2.8	156.3/154.5/108.1/107.6	
3,5-diOHBA	154.12	$C_7H_6O_4$	6.78	2&6 / 2H	d / 2.2	167.4/158.4/107.3/106.8	By-product of authentic 2-Cl-3,5-diOHBA
			6.39	4 / 1H	t / 2.2	158.4/107.3w	
2,3,5-triOHBA	170.12	$C_7H_6O_5$	6.59	6 / 1H	d / 2.9	172.3/148.9w/143.7/109.8	
			6.51	4 / 1H	d / 2.9	148.9w/146.4w/143.7/104.2	
Chelidonic acid	184.10	$C_7H_4O_6$	6.91	3&5/ 2H	s	160.9/154.1/119.1	

[a] s= singlet, d = doublet, t = triplet, m = multiplet.

[b] Isolated compound F was measured in D_2O/DMSO 5/1.

Table S3. ^{13}C NMR chemical shift assignments in methanol-d4 and DMSO-d6 solutions of detected isolated metabolites and authentic compounds. Numbering of carbon atoms for all compounds is shown in Figure S3.

compound / $\delta^{13}C$ (ppm)	C-1	C-2	C-3	C-4	C-5	C-6	C-7	Remark
methanol-d_4								
Isolated metabolites								
2,6-diCl-3-OHBA	136.8	118.8	153.9	118.5	129.5	121.1	168.1	Produced by M6$_{bbdD}$
Compound A	140.2	108.6	154.0	104.3	154.0	108.6	170.3	Produced by MSH1 wt
Compound C	120.6	118.6	142.5	147.5	115.2	131.2	170.9	Produced by MSH1 wt
Authentic compounds								
2,6-DCBA	136.0	132.2	129.1	132.1	129.1	132.2	167.7	Substrate for M6$_{bbdD}$ cells
2,6-diCl-3-OHBA	136.8	118.8	153.9	118.5	129.5	121.1	168.1	Substrate for MSH1 wt
2,6-diCl-3,5-diOHBA	137.1	108.8	154.2	105.3	154.2	108.8	168.5	
2-Cl-3,5-diOHBA	134.1	110.7	155.8	107.1	157.8	109.6	169.8	
3,5-diOHBA	133.6	109.0	159.7	108.1	159.7	109.0	170.0	By-product of authentic 2-Cl-3,5-diOHBA
DMSO-d_6								
Isolated metabolites								
Compound B	n.d.	107.8	154.8	104.9	156.3	107.2	168.1	Produced by MSH1 wt
Compound D	112.4	143.6	146.4	109.8	148.9	104.1	172.3	Produced by purified BbdC
Compound F[(a)]	161.1	165.5	117.5	185.7	117.5	165.5	161.1	Produced by M6$_{bbdF}$ extract
Authentic compounds								
2-Cl-3,5-diOHBA	133.6	108.1	154.5	105.5	156.3	107.6	167.3	
3,5-diOHBA	132.5	107.3	158.4	106.8	158.4	107.3	167.4	By-product of 2-Cl-3,5-diOHBA
2,3,5-triOHBA	112.5	143.7	146.4	109.8	148.9	104.2	172.3	
Chelidonic acid	160.9	154.1	119.1	179.4	119.1	154.1	160.9	

[a] Isolated compound F was measured in D_2O/DMSO 5/1.

References

(1) Breugelmans, P.; Leroy, B.; Bers, K.; Dejonghe, W.; Wattiez, R.; De Mot, R.; Springael, D. Proteomic study of linuron and 3,4-dichloroaniline degradation by *Variovorax* sp. WDL1: evidence for the involvement of an aniline dioxygenase-related multicomponent protein. *Res. Microbiol.* **2010**, *161* (3), 208–218. https://doi.org/10.1016/j.resmic.2010.01.010.

(2) Warner, J. R.; Copley, S. D. Pre-steady-state kinetic studies of the reductive dehalogenation catalyzed by tetrachlorohydroquinone dehalogenase. *Biochemistry* **2007**, *46* (45), 13211–13222. https://doi.org/10.1021/bi701069n.

(3) Tully, B. J.; Wheat, C. G.; Glazer, B. T.; Huber, J. A. A dynamic microbial community with high functional redundancy inhabits the cold, oxic subseafloor aquifer. *ISME J.* **2018**, *12* (1), 1–16. https://doi.org/10.1038/ismej.2017.187.

(4) Chan, W. Y.; Wong, M.; Guthrie, J.; Savchenko, A. V.; Yakunin, A. F.; Pai, E. F.; Edwards, E. A. sequence- and activity-based screening of microbial genomes for novel dehalogenases. *Microb. Biotechnol.* **2010**, *3* (1), 107–120. https://doi.org/10.1111/j.1751-7915.2009.00155.x.

(5) Shen, Z.-W.; Fisinger, U.; Poulev, A.; Eisenreich, W.; Werner, I.; Pleiner, E.; Bacher, A.; Zenk, M. H. tracer studies with 13C-labeled carbohydrates in cultured plant cells. retrobiosynthetic analysis of chelidonic acid Biosynthesis. *Phytochemistry* **2001**, *57* (1), 33–42. https://doi.org/10.1016/S0031-9422(00)00496-9.